Developmentally regulated *tcf7l2* splice variants mediate transcriptional repressor functions during eye formation

Rodrigo M. Young[1*], Kenneth B. Ewan[2], Veronica P. Ferrer[1], Miguel L. Allende[3], Trevor C. Dale[2], Stephen W. Wilson[1*].

1. Department of Cell and Developmental Biology, UCL, Gower St, London WC1E 6BT, UK

2. School of Bioscience, Cardiff University, Cardiff, CF10 3AX, UK

3. FONDAP Center for Genome Regulation, Facultad de Ciencias, Universidad de Chile, Casilla 653, Santiago, Chile.

* Correspondence: rodrigo.young@ucl.ac.uk or s.wilson@ucl.ac.uk

Running Title: *tcf7l2* splicing impacts eye development

Keywords: alternative splicing/eye development/Tcf7l2/Wnt/zebrafish

Abstract

Tcf7l2 mediates Wnt/β-Catenin signalling during development and is implicated in cancer and type-2 diabetes. The mechanisms by which Tcf7l2 and Wnt/β-Catenin/Tcf signalling more generally elicits such a diversity of biological outcomes are poorly understood. Here, we identify an alternatively spliced *tcf7l2* exon5 and show that only splice variants that include this exon provide compensatory repressor function to restore eye formation in zebrafish embryos lacking *tcf7l1a/b* function. Knockdown of *tcf7l2* variants that include exon5 in *tcf7l1a* mutants also compromises eye formation and these variants can effectively compete with constitutively-active human *VP16*-TCF7L2 in reporter assays using Wnt target gene promoters. We show that the repressive activities of exon5 coded variants are likely explained by their higher affinity for Tle co-repressors. Furthermore, putatively phosphorylated residues in Tcf7l2 coded exon5 facilitate repressor activity. Our studies suggest that regulation of *tcf7l2* splicing influences the level of transcriptional repression mediated by Wnt pathway.

Introduction

Wnt signalling has a broad array of biological functions, from regional patterning and fate specification during embryonic development to tissue homeostasis and stem cell niche maintenance in adult organs (van Amerongen and Nusse, 2009, Nusse and Clevers, 2017). Because of its relevance to such a diversity of processes, Wnt pathway misregulation is linked to a range of diseases such as cancer, diabetes and neurological/behavioural conditions (Nusse and Clevers, 2017). Wnt can activate several intracellular pathways, and the branch that controls gene expression works specifically through β-catenin and the small family of T-Cell transcription factors (Tcfs; Cadigan and Waterman, 2012).

In absence of Wnt ligand, intracellular β-catenin levels are kept low by a mechanism that involves phosphorylation by GSK3β and CK1α, which is mediated by the scaffolding of β-catenin by Axin1 and APC in what is termed the destruction complex (MacDonald and He, 2012, Niehrs, 2012). Phosphorylated β-catenin is ubiquitilated and degraded in the proteasome (MacDonald et al., 2009, Niehrs, 2012). In this context, Tcf transcription factors actively repress the transcription of downstream genes by interacting with Gro/TLE like co-repressors (Cadigan and Waterman, 2012, Hoppler and Waterman, 2014). When cells are exposed to Wnt ligand, the destruction complex is disassembled and β-catenin is no longer phosphorylated and committed to degradation (MacDonald et al., 2009, Niehrs, 2012). This promotes the translocation of β-catenin to the nucleus where it displaces co-repressors by its interaction with Tcfs, activating the transcription of Wnt target genes (Cadigan and Waterman, 2012, Hoppler and Waterman, 2014, Schuijers et al., 2014). Hence, Tcf proteins are thought to work as transcriptional switches that can activate transcription in presence of Wnt ligand or repress transcription in its absence.

During development, ensuring appropriate levels of Wnt/β-catenin signalling is essential for many processes. For instance, during gastrulation, specification of the eyes and telencephalon can only occur when Wnt/β-catenin signalling is low or absent and overactivation of the pathway in the

anterior neuroectoderm mispatterns the neural plate leading to embryos with no eyes (Kim et al., 2000, Heisenberg at al., 2001, Kiecker and Niehrs, 2001, Houart et al., 2002). Illustrating this, fish embryos mutant for *axin1*, a member of the β-catenin destruction complex, are eyeless because cells fail to phosphorylate β-catenin, leading to abnormally high levels of the protein, mimicking a Wnt active state (Heisenberg et al, 2001). Similarly, maternal-zygotic *tcf7l1a/headless* mutants also mimick Wnt/β-catenin overactivation and are eyeless (Kim et al., 2000) suggesting that it is necessary to actively repress Wnt/β-catenin target genes for regional patterning to occur normally (Kim et al., 2000, Nguyen et al., 2009).

In vertebrates, Lef/Tcf transcription factors constitute a family of four genes: *lef1*, *tcf7(tcf1)*, *tcf7l1(tcf3)* and *tcf7l2(tcf4)*. All contain a highly conserved β-catenin binding domain (β-catenin-BD) at the N-terminal end and a high mobility group box (HMG-box) DNA binding domain (DNA-BD) in the middle of the protein (Fig. 1A, Cadigan and Waterman, 2012, Hoppler and Waterman, 2014). All Tcf proteins bind the 5'-CCTTTGATS-3' (S=G/C) DNA motif, but can also bind to sequences that diverge from this consensus (van de Wetering et al., 1997, van Beest et al., 2000, Hallikas et al., 2006, Atcha et al., 2007). The fact that all Tcfs bind to the same motif has led to the notion that the functional specificity of Lef/Tcf proteins may be imparted by inclusion or exclusion of functional motifs by alternative transcription start sites or alternative splicing (Hoppler and Waterman, 2014).

The region in between the β-catenin-BD and the DNA-BD of Lef/Tcf proteins, known as the context-dependent regulatory domain (CDRD), and the C-terminal end of the protein, are coded by alternatively spliced exons (Fig. 1A, Archbold et al., 2012, Cadigan and Waterman, 2012, Hoppler and Waterman, 2014). The C-terminal region of Lef/Tcfs includes the C-Clamp domain and two CtBP interacting motifs (Fig. 1A, Brannon et al., 1999, Valenta et al., 2003, Atcha et al., 2007, Hoverter et al., 2012, Hoverter et al., 2014). In certain contexts, the C-clamp domain helps DNA binding and increases the selectivity for certain gene promoters (Atcha et al., 2007, Wohrle et al.,

2007, Chang et al., 2008, Weise et al., 2010). The CDRD includes the domain of interaction with Gro/TLE co-repressors (GBS, Fig. 1A, Cavallo et al., 1998, Roose et al., 1998, Daniels and Weis, 2005, Arce et al., 2009, Chodaparambil et al., 2014) and amino acids that can promote Lef/Tcf dissociation from DNA, modify nuclear localisation or promote activation of transcription when phosphorylated by HIPK2, TNIK or NLK (Shetty et al., 2005, Mahmoudi et al., 2009, Hikasa et al., 2010, Ota et al., 2012). Exons 4 and 5 and the borders of exon7 and exon 9 that are included in the CDRD region are alternatively spliced in *tcf7l2* (Duval et al., 2000, Pukrop et al., 2001, Young et al. 2002). The inclusion of the border of exon 9 can transform Tcf7l2 into a strong transcriptional repressor (Liu et al., 2005). Hence, splicing regulation in the CDRD could, similarly, be relevant to transcriptional output (Tsedensodnom et al., 2011, Koga et al., 2012). However, the function of the alternatively spliced exons 4 and 5 is still unknown. All such variations in Lef/Tcf proteins may contribute to their functional diversity, an idea that is supported by the fact that Tcfs control many different subsets of genes (Cadigan and Waterman, 2012, Hrckulak et al., 2016).

In this study, we address the role of alternative splicing in mediating the functional properties of Tcf7l2 during early nervous system development. Tcf7l2 has various known roles including a requirement during establishment of left-right asymmetry in the forebrain and for the maintenance of the stem cell compartment in colon and skin epithelia (Korinek et al., 1998, Nguyen et al., 2009, Hüsken et al., 2014). Additionally, polymorphisms in the genomic region that codes for human *tcf7l2* exon4 segregate with acquisition of type-2 diabetes (Grant et al., 2006), and conditional knockdowns of *tcf7l2* give rise to mice with phenotypes comparable to diabetic patients (Boj et al., 2012). *tcf7l2* has an alternative translation start site and alternative splicing in the CDRD and in exons that lead to shorter C-terminal ends (Duval et al., 2000, Young et al., 2002, Vacik et al., 2011). This suggests that many regulatory inputs could influence the transcriptional output of Tcf7l2.

Our results show that alternative splicing of *tcf7l2* significantly impacts the transcriptional repressor activity of the encoded protein. *tcf7l2* splice variants have been characterised in humans and, to a lesser extent, in mice and zebrafish (Duval et al., 2000, Young et al., 2002, Prokunina-Olsson et al., 2009, Weise et al., 2010) but little information is available on different roles for the splice variants. In zebrafish, *tcf7l2* is first expressed in the anterior neuroectoderm by the end of gastrulation (Young et al., 2002) and in this study, we show that at this stage, *tcf7l2* is only expressed as long C-terminal variants that can include a newly identified alternative exon 5. We show that only Tcf7l2 variants that include the coded exon 5 are able to provide the repressive function required for eye specification. Moreover, only these variants effectively repress Wnt target gene promoters in luciferase assays, probably due to their higher affinity with Tle co-repressors. We further show that two putatively phosphorylated amino acids coded by exon 5 of Tcf7l2 are required for this interaction, and overall repressive function. Hence, alternative exon 5 in zebrafish *tcf7l2* seems to play a critical role in mediating transcriptional repression of Wnt downstream genes. Our data suggest that through inclusion of the region coded by exon 5, Tcf7l2 could be part of a phosphorylation regulatory module that keeps Wnt pathway in an 'off' state by phosphorylating β-catenin in the cytoplasm and Tcf7l2 in the nucleus.

Results

Characterisation of a novel *tcf7l2* alternative splice variant.

With the aim of addressing the functional roles of different *tcf7l2* splice forms, we first cloned the zebrafish splice forms affecting the CDRD region (Fig. 1A). This region of Tcf proteins is close to the fragment that interacts with Gro/TLE like co-repressors (GBS, Fig. 1A) and consequently alternative splice forms may affect transcriptional function (Duval et al., 2000, Young et al., 2002, Roose et al., 1998, Daniels and Weis, 2005). Using primers flanking the region containing putative alternative

exons in the CDRD encoding region (Primer set-a, Fig. 1A), we performed RT-PCR and cloned the resulting-DNA fragments.

The amplified DNA contained a new exon not previously described in zebrafish or in any other species (Fig. 1B, Fig. S1, accession no xxxxx). This exon (*tcf7l2* exon 5 hereafter) codes for 20 amino acids and is flanked by consensus splice acceptor and donor intron sequences. Human *tcf7l2* exons 3a and 4a are alternatively spliced exons in this region (Fig. 1D, Prokunina-Olsson, 2009). Zebrafish *tcf7l2* exon 5 is similar in size to human *tcf7l2* exon 3a but instead lies in a genomic location that in the human gene would be positioned between exons 4 and 5, where alternative human exon 4a is located (Fig. 1D). Although sequence homology with other fish species is high (Fig. 1B, Fig. S2A), the amino acid identity encoded by human exon 3a and zebrafish exon 5 is only 33% (Fig. 1C). However, in both species all neighbouring exons are the same size, show a high degree of homology at the nucleotide and protein level and are surrounded by long introns (Fig. 1D, Fig. S2B). Moreover, both fish and human exons 5/3a encode residues that are putative CK1/PKA kinase phosphorylation sites (Fig. 1B, C, asterisks).

RT-PCR experiments show that splice variants that include exon 4 are expressed maternally and zygotically (Fig1E, upper panel, middle band labelled '4 or 5', asterisk). Exon 5 is expressed zygotically and is included in variants that include exon 4 from 6hpf (hours post fertilisation, Fig. 1E, upper panel, top band labelled '4 and 5'). *tcf7l2* splice variants that include exon 5 and lack exon 4 and that lack both exons 4 and 5 (Fig. 1E, upper panel, lower band labelled 'none') are expressed from 48hpf.

We characterised additional splice forms, by analysing the 5' alternative splice end of *tcf7l2* exon 15 for the presence of long, medium or short splice variant C-terminal (Ct) ends (Fig. 1A,E, lower panel). The inclusion of two alternative forms of exon 15 border in this region adds a premature stop codon that leads to medium and short Tcf7l2 Ct variants respectively (Young et al., 2002). Maternally, and until 24hpf, *tcf7l2* is only expressed as transcripts that lead to long (L) Tcf7l2

variants (Fig. 1E, bottom panel, lower band). From 48hpf onwards *tcf7l2* is predominantly expressed as splice forms that code for medium (M) and short (S) Ct Tc7f7l2 variants, with L variants barely detectable (Fig. 1E, bottom panel, top two bands).

We further assessed how the expression of exons 4 and 5 relate to alternative splice forms in exon 15 affecting the Ct domain of Tcf7l2. Before 48hpf, *tcf7l2* is only expressed as splice forms that lead to L Ct variants but from 48hpf, variants including exon 4 are expressed mainly as splice variants that code for M but also as S and L Ct-forms (Fig. S3A). On another hand, at 48hpf and onwards, transcripts including exon 5 are expressed as M or S Tcf7l2 Ct-variants and by 96hpf only as M variants (Fig. S3B). The range of Tcf7l2 variants expressed as development proceeds is summarised in Table S1A and B.

Given the functional relevance of Tcf7l2 in adult tissue homeostasis (Nusse and Clevers 2017), we studied splicing events involving exons 4/5 and exon 15 in adult zebrafish eye, brain, gut, liver, pancreas, ovaries and testis (Fig. S3C-F). A summary of the RT-PCR results and Tcf7l2 variants expressed in adult organs based on this RT-PCR data is presented in Table S2A and B.

From here, we focus on *tcf7l2* splice variants expressed as the anterior neuroectoderm is patterned during gastrula and early somite stages.

***tcf7l2* is broadly expressed in the anterior neural plate.**

The analyses above show that by early somite stage (12hpf), *tcf7l2* is predominantly expressed as two long Ct isoforms, all of which include exon 4. One of these is expressed maternally and zygotically, that lacks exon 5 (4L variants), and the other is expressed zygotically and includes exon 5 (45L variants).

From late gastrula stage, *tcf7l2* is expressed in the anterior neural plate (Young et al., 2002), overlapping-*tcf7l1a* and *tcf7l1b* (Kim et al., 2000, Dorsky et al., 2003). Expression rostrally overlaps with that of *emx3* (Fig1F, Morita et al., 1995) delimiting the prospective telencephalon and the caudal boundary of *tcf7l2* expression is rostral to that of midbrain markers (*pax2.1* Fig. 1G).

Consequently, *tcf7l2* is expressed throughout most of the prospective forebrain including the eye field during the stages when the neural plate becomes regionalised into discrete domains.

tcf7l2 mutants have smaller eyes.

The *m881* mutant allele of *tcf7l1a* adds a new splice site in intron 7 which leads to a frame shift in the reading frame (Kim et al., 2000). The use of this new splice site is fully penetrant and as the premature stop codon induces nonsense mediated decay of the transcript, *m881* is consequently predicted to be a null allele (Young and Wilson, Unpublished). Zygotic *tcf7l1a/headless*$^{m881/m881}$ mutants (*tcf7l1a*$^{-/-}$ from here onwards) show reduced eye size at 30hpf, but are viable and fertile (Fig. 2G, Table S5, Kim et al., 2000). In the *zf55* (*exl*) allele of *tcf7l2* the first intron of the gene is retained into the mRNA which knocks down expression of the protein generated by the reading frame starting in exon 1 (Muncan et al., 2007). We find that homozygous *tcf7l2*^{zf55} mutants also have reduced eye size at 30hpf (Fig. 2B, G, Table S5, having an *en face* eye profile 47% of the size of wildtype siblings, n=7), comparable to the 64% reduction in *tcf7l1a*$^{-/-}$ mutants (Fig. 2G).

When *tcf7l1b*, the onologue of *tcf7l1a,* function is impaired by injecting 0.12pmol of a validated ATG morpholino (mo^{tcf7l1b}) in *tcf7l1a* mutants, eyes fail to be specified due to loss of repressor activity (Fig. 2D, Table S3, Dorsky et al., 2003). To assess if *tcf7l2* may also functionally compensate for loss of *tcf7l1a,* we incrossed double heterozygous *tcf7l1a*$^{+/m881}$/*tcf7l2*$^{+/zf55}$ fish. However, we did not observe an eyeless phenotype in *tcf7l1a/tcf7l2* double homozygous mutants (Fig. 2C, G).

Exon 5 of _tcf7l2_ is required to rescue eye formation upon loss of _tcf7l1a/b_ function.

To address whether there are any functional differences between *tcf7l2* splice variants with or without exon 5 expressed at 12hpf (both with long C-terminal ends (Fig. 1E, Table S1B)), we assessed their respective abilities to rescue eye formation when Tcf7l1a/Tcf7l1b function was abrogated (Fig. 2D). Embryos from *tcf7l1a*$^{+/-}$ female to *tcf7l1a*$^{-/-}$ male crosses were co-injected with 0.12pmol of mo^{tcf7l1b} and 20pg of either *4L-tcf7l2* or *45L-tcf7l2* mRNAs. Control

overexpression of these *tcf7l2* variants did not induce any phenotype in wildtype or *tcf7l1a*$^{+/-}$ embryos (not shown).

Exogenous *45L-tcf7l2* mRNA rescued the eyeless phenotype in *tcf7l1a*$^{-/-}$/*tcf7l1b* morphant embryos whereas *4L-tcf7l2* mRNA did not (Fig. 2E, H, TableS4, 89%, n=326 embryos, 3 experiments). This suggests that only *tcf7l2* splice variants that include exon 5 could contribute together with *tcf7l1a/b* to the process of eye formation.

An alternative explanation for the poor rescue by the 4L-Tcf7l2 variant could be that it is either not localised to the nucleus or has lower protein stability. To address this, we transfected HEK293 cells with constructs encoding N-terminal Myc tagged constructs of Tcf7l2. Both Tcf7l2 variants were expressed and localised to the nucleus (Fig. S4), suggesting that the lack of rescue with *4L-tcf7l2* mRNA is due to other differences in protein function. The myc-tagged Tcf7l2 variants are also able to rescue the eyeless phenotype in *tcf7l1a*$^{-/-}$ mutants injected with mo^{tcf7l1b} to the same extent as untagged variants (Fig. 2H; TableS4).

To address if the *45L-tcf7l2* splice variant plays a role in eye formation, we injected 1.25pmol/embryo of a splicing morpholino (mo^{SPtcf7l2}) that targets the intron/exon splice boundary 5' to exon5 (Fig. S5A). This is predicted to force the splicing machinery to skip exon5 and splice exon4 to exon6, such that only 4L-Tcf7l2 variants would be translated. This was confirmed by RT-PCR, which shows that the band corresponding to *45L-tcf7l2* mRNA is absent in mo^{SPtcf7l2} morphants, but *4L-tcf7l2* mRNA is still present (Fig. S5B). Sequencing of the putative *4L-tcf7l2* band shows that the exon4/6 splicing event in mo^{SPtcf7l2} injected morphants is in frame and only leads to the expression of the *4L-tcf7l2* variant (not shown). As expected, Tcf7l2 protein is still present when detected by Western blot (FigS5B).

Injection of mo^{SPtcf7l2} in *tcf7l1a*$^{-/-}$ mutants leads to a fully penetrant eyeless phenotype (Fig. 2F, H, Table S3, n=127 of 127, three independent experiments). No phenotype was observed when mo^{SPtcf7l2} was injected in sibling heterozygous embryos (Table S3) or when a scrambled control

morpholino (moC) was injected in *tcf7l1a*$^{-/-}$ mutants (not shown). This suggests that 45-Tcf7l2 variants and not 4L-Tcf7l2 variants can compensate for loss of Tcf7l1a/b in eye specification. This finding is perhaps surprising given that we did not observe an eyeless phenotype in *tcf7l1a*$^{-/-}$*/tcf7l2*$^{zf55/zf55}$ embryos. Possible reasons for the different phenotypes are elaborated in the Discussion.

Tcf7l2 splice variant with exon 5 shows repressor activity in luciferase reporter assays.

As Tcf transcription factors mediate Wnt/β-catenin signalling (Hoppler and Waterman, 2014), the differential functions of the two Tcf7l2 variants could potentially be explained by their ability to activate/repress the transcription of different subsets of genes. To explore whether the Tcf7l2 variants show differing promoter transactivation abilities, we performed luciferase assays using the generic TOPflash reporter and promoters of the Wnt pathway regulated genes, *cdx1* (Hecht and Stemmler, 2003), *engrailed* (McGrew et al., 1999), *cJUN* (Nateri et al., 2005), *lef1* (Hovanes et al., 2001) and *siamois* (Brannon et al., 1999). All the promoters of these genes used in the luciferase assays contain consensus Tcf binding elements.

HEK293 cells were transiently transfected with the luciferase reporter construct and DNA encoding for a constitutively-active VP16-TCF7L2 fusion protein, which induces expression at Wnt-responsive promoters in absence of nuclear β-catenin (Ewan et al., 2010). As expected, all the tested reporters show a strong response to VP16-TCF7L2 (Fig. 3A-F, second bar in all plots). We then assessed whether Tcf7l2 splice variants with or without exon 5 could influence transactivation of the luciferase reporters by co-transfecting *VP16-TCF7L2* with either *4L-tcf7l2* or *45L-tcf7l2* splice variants.

Neither the 4L-Tcf7l2 or 45L-Tcf7l2 variants were able to compete significantly with VP16-TCF7L2 when tested with the *cjun* promoter (Fig. 3C). However, 45L-Tcf7l2 shows a greater ability to compete with VP16-TCF7L2 when tested with *cdx1*, *engrailed*, *lef1*, *siamois* and TOPFlash

reporters (Fig. 3A,B,D,E,F). This suggests that Tcf7l2 variants including exon5 are able to repress transcription of certain promoters by out-competing dominant active VP16-TCF7L2.

Inclusion of exon 5 enhances the interaction between Tcf7l2 and Tle3b

The region of Tcf7l2 encoded by exon 5 is located in the vicinity where Lef/Tcf proteins interact with Gro/TLE-like corepressors (Roose et al., 1998, Brantjes at el., 2001, Daniels and Weis, 2005, Arce et al., 2009). Consequently, exon 5 could potentially assign promoter-specific repressor activity by mediating the interaction of Tcf7l2 with Gro/TLE proteins. Alternatively, inclusion of exon 5 could modify the capacity of Tcf7l2 to interact with transactivating β-catenin.

To address if exon5 modulates interactions between Tcf7l2 and Gro/TLE or β-catenin proteins, we performed yeast two-hybrid (Y2H) protein interaction experiments between 4L-Tcf7l2 and 45L-Tcf7l2 variants and Tle3b (the zebrafish orthologue of mammalian Tle3/Gro1), or β-catenin (Fig. S6). Full-length Tle3b seemed to either be toxic or have transfection problems in the yeast strain and so we used a C-terminal deletion of Tle3b (dC-Tle3b), which still included the glutamine-rich domain that interacts with Tcf proteins (Daniels and Weis, 2005). Yeast co-transfected with *β-catenin* or *tle3b* and *4L-tcf7l2* or *45L-tcf7l2* splice variants are able to grow in complete auxotrophic selective media (-L-A-H-W + Aureoblastinin) and also express the X-gal selection reporter (Fig. S6). This suggests that both Tcf7l2 variants are able to interact with β-catenin and dC-Tle3b. However, Y2H assays do not reveal differences in the affinity of interactions between proteins.

To address possible differences in protein affinity between Tcf7l2 and β-catenin or Tle3b, we performed co-immunoprecipitation (co-IP) experiments using extracts from HEK293 cells. Both Myc tagged Tcf7l2 variants were efficiently immunoprecipitated by anti-myc beads (Fig. 4, right top panel) and showed a similar capacity to co-IP with β-catenin (Fig. 4, right middle panel, second and third lanes). However, 45L-Tcf7l2 shows a significantly higher capacity to co-IP Tle3b compared to 4L-Tcf7l2 (Fig. 4, right bottom panel, second and third lane, asterisk). This suggests

that the repressor activity of 45L-Tcf7l2 could be mediated by a more effective interaction with Gro/TLE-like co-repressors.

Putatively phosphorylated amino acids in the domain of Tcf7l2 coded by exon 5 mediate transcriptional repression

Kinases are known to modulate Wnt signalling activity through phosphorylation of LRP6, β-catenin and Tcfs (Li et al., 2002, Davidson et al., 2005, Zeng et al., 2005, Sokol, 2011) and bioinformatic analysis using GPS2.0 predicts that Tcf7l2 exon 5 coded threonine 172 and serine 175 are putatively phosphorylatable by CK1, PKA, and other kinases (http://gps.biocuckoo.org/, Xue et al., 2008). CK1 is known to regulate Wnt signalling by phosphorylating LRP6 co-receptor and β-catenin (Niehrs, 2012).

To address the role of these amino acids in Tcf7l2 we generated a 45L-Tcf7l2 mutant version (45L-Tcf7l2-AA) in which both threonine p.172 and serine p.175 were replaced by alanine, which cannot be phosphorylated. Unlike *45L-tcf7l2*, expression of *45L-tcf7l2-AA* is unable to rescue the eyeless phenotype of *tcf7l1a*$^{-/-}$*/tcf7l1b* morphant embryos (Fig. 2H, Table S4). Moreover, 45L-Tcf7l2-AA behaves like 4L-Tcf7l2 variants in luciferase assays (Fig. 3, fifth bar in all plots), and also shows a reduced capacity to interact with Tle3b in co-IP experiments (Fig. 4, right bottom panel, fourth lane). Of note, the Tcf7l2-AA mutant shows stronger co-IP with β-catenin compared to 4L-Tcf7l2 or 45L-Tcf7l2 variants (Fig. 4, right top panel, fourth lane). These results suggest that phosphoserine and phosphothreonine residues may regulate the ability of 45L-Tcf7l2 to repress target genes and consequently contribute to eye specification.

Discussion

In this study, we show that developmentally regulating splicing contributes to Wnt signalling during patterning of the anterior neural plate and eyes. We show that there is extensive variety in splicing of zebrafish Tcf7l2 throughout development and across adult tissues and that the exon 5

coded region within Tcf7l2 influences transcriptional repression function. This function is required for maintaining low levels of pathway activity during forebrain and eye specification. We show that long-Ct Tcf7l2 variants that include both exons 4 and 5 can rescue eye formation in fish with compromised *tcf7l1a/b* function, *tcf7l2* homozygous mutants develop smaller eyes and specific knockdown of the 45L-Tcf7l2 variant in *tcf7l1a* mutants leads to embryos with no eyes. Additionally, 45L-Tcf7l2 variants can out-compete constitutively transcriptionally active VP16-hTcf7l2 chimeras at promoters of known Wnt target genes in luciferase reporter assays. Our results also suggest that the function of the 45L-Tcf7l2 variant could be mediated by its phosphorylation in the exon 5-coded region and that this putative phosphorylation event may enable its interaction with Tle3b corepressor to mediate transcriptional repression.

Tcf7l2 transcriptional repression function is required for forebrain patterning

Like *tcf7l1a* and *tcf7l1b*, *tcf7l2* is expressed in the anterior neural ectoderm, from where the eyes and forebrain develop (Kim et al., 2000, Young et al., 2002, Dorsky et al., 2003). Experimental manipulations or mutations that increase Wnt/β-catenin activity in the anterior neural plate during gastrulation generate embryos with no forebrain and eyes (Wilson and Houart, 2004). For instance zebrafish embryos lacking zygotic *tcf7l1a/headless*^{m881} function have smaller eyes (Kim et al., 2000), a phenotype that is exacerbated when *tcf7lb* is knocked down in *tcf7l1a* mutants (Dorsky et al., 2003). The notion that active repression by Tcf7l1a/b transcription factors is required for neuroectodermal patterning is supported by the observation that overexpression of transcriptional dominant active *VP16-tcf7l1a* chimera also leads to eyeless embryos (Kim et al., 2000).

Eyes in homozygous *tcf7l2* mutant embryos are smaller suggesting that, like *tcf7l1* genes, the transcriptional repressive function of this transcription factor contributes to forebrain patterning and eye formation. As only the 45L-Tcf7l2 variant, that includes exon5 is able to rescue forebrain specification in *tcf7l1a*$^{-/-}$*;tcf7l1b* morphant embryos, we suggest that exon5 assigns transcriptional

repressor function to Tcf7l2. This is supported by finding greater repressor activity of 45L-Tcf7l2 variants compared to 4L-Tcf7l2 that lacks the exon 5 coded region in luciferase reporter experiments and by the fact that 45L-Tcf7l2 variants show greater association for Tle3b transcriptional co-repressor in co-IP experiments.

The lack of severe forebrain and eye phenotypes in single *tcf7l1* mutants is at least in part due to the overlapping functional activities of different *tcf* genes and we assume the same is likely for the *tcf7l2* mutant. However, our study raises the likelihood that additional levels of genetic regulation may influence expressivity of developmental phenotypes. Given the Tcfs have both repressor and activator roles, mutations that disrupt the balance between these roles may lead to phenotypes differing from complete abrogation; one would predict mis-regulation of repressor function while maintaining the ability of the protein to activate transcription (as predicted in our experiments to knock down *45L-tcf7l2* variants with a splicing morpholino) might lead to more severe forebrain and eye phenotypes than complete loss of protein function.

Phosphorylation of Tcf7l2 may mediate its transcriptional repressor function.

Tcfs can be acetylated, phosphorylated and sumoylated in the context dependent regulatory domain (CDRD), which includes the region coded by *tcf7l2* exon 5 (Yamamoto et al., 2003, Shetty et al., 2005, Mahmoudi et al., 2009, Hikasa et al., 2010, Ota et al., 2012, Elfert et al., 2013). The importance of phosphorylation to the repressor activity of Tcf7l2 is suggested by the finding that the phosphorylation resistant Tcf7l2-AA mutant form in which both amino acids p.172 and p.175 are replaced by alanine, behaves as if lacking the region coded by exon 5 in all functional assays. Gro/TLE transcription co-repressors are displaced by β-catenin to allow Tcf-mediated transcriptional activation (Daniels and Weis 2005, Arce et al., 2009, Chodaparambil et al., 2014) and although we find 45L-Tcf7l2 still interacts with β-catenin, the Tcf7l2-AA mutant variants shows higher affinity binding. This raises the possibility that 45L-Tcf7l2 variants may co-exist as phosphorylated and un-phosphorylated pools with different repressor/activator activity.

It is widely accepted that Tcfs work as transcriptional switches, repressing transcription of downstream genes in absence of Wnt ligand, and turning on gene transcription when Wnt signalling is active (Cadigan, 2012). In this context, the repressive function of Tcf7l2 may be part of an integrated pathway response when the Wnt pathway is not active. The 'off' state of Wnt signalling involves active phosphorylation of β-catenin by CK1α and GSK3b kinases (MacDonald and He, 2012, Niehrs, 2012). Our findings support a model in which Tcf transcription factors could also be part of a kinase regulatory module that maintains the pathway in an 'off' state, not only in the cytoplasm by phosphorylating β-catenin, but also by promoting transcriptional repression through phosphorylation of Tcf7l2. Direct assessment of an *in vivo* functional role for phosphorylation of Tcf7l2, and potentially other Tcfs, will be needed to address this idea.

The salience of resolving a role for phosphorylation in the regulation of transcriptional activation/repression is heightened given the relevance of Tcf7l2 in mediating colorectal cancer outcome due to imbalanced Wnt signalling. Indeed, one future avenue for investigation will be to identify proteins that interact with the phosphorylated and un-phosphorylated forms of Tcf7l2.

Functional modulation of Tcf7l2 through spatial and temporal regulation of splicing of alternative exons

The occurrence of widespread tissue specific and developmentally regulated Tcf7l2 splicing suggests that specific variants of Tcf7l2 are required for proper tissue specification both during development and for its various roles in organ function during adult life (Nusse and Clevers, 2017). For instance, we have previously shown that Tcf7l2 is required for the development of left-right asymmetry of habenular neurons (Hüsken et al., 2014) and at the stages during which the habenula is developing its laterality traits, *tcf7l2* splice variants transition from all expressing long Ct-ends to only medium and short variants. This is potentially significant as only long variants include a complete C-clamp DNA binding-helper domain (Young et al., 2002) and this domain can direct Tcf7l2 to specific promoters (Hoverter et al., 2014). Consequently, absence of a whole C-

clamp may bias the promoter occupancy of Tcf7l2 and shift the expression profile of Wnt downstream genes (Atcha et al., 2003, 2007, Hecht and Stemmler, 2003, Hoveter et al., 2014).

Tcf7l2 is linked to type-2 diabetes outcome (Grant et al., 2006, Lyssenko et al., 2007, Prokunina-Olsson et al., 2009, Savic et al., 2011) and the strongest risk factor SNPs are located in introns flanking human *tcf7l2* genomic exon 4a (Grant et al., 2006). Perhaps surprisingly only liver tissue-specific *tcf7l2* knockouts in mice and not other organs (including pancreas), lead to metabolic outcomes mimicking type-2 diabetes (Boj et al., 2012 and see Bailey et al., 2015). Adult zebrafish liver only expresses 4L and 45L Tcf7l2 variants. Although homologies between fish and human exons in this region of Tcf7l2 are uncertain and despite lack of overall sequence conservation, human *tcf7l2* exon 4 and fish exon 5 have a similar size and share amino acids that are phosphorylated in zebrafish Tcf7l2 coded exon 5. This suggests that the region coded by human Tcf7l2 exon 4 and fish exon 5 may have similar functions. Consequently, it will be interesting to assess if the expression levels of human *TCF7L2* exons analogous to zebrafish *tcf7l2* exons 4/5 is altered in the liver of type-2 diabetes patients carrying risk factor SNPs.

Given the importance of maintaining balanced Wnt/β-catenin pathway activity throughout development and tissue homeostasis, elucidating all mechanisms that impact Wnt signalling modulation is critical if we are to understand, and develop ways to manipulate, pathway activity when mis-regulated in pathological conditions. Our work adds weight to the idea that alternative splicing and controlling the balance between repressor and activator functions is an important route for pathway regulation.

Materials and Methods

Animal use, mutant and transgene alleles, genotyping and quantification of eye profile size: Adult zebrafish were kept under standard husbandry conditions and embryos obtained by natural spawning. Wildtype and mutant embryos were raised at 28ºC and staged according to Kimmel et al. (1995). Fish lines used were *tcf7l1a*^{m881} (Kim et al., 2000), *tcf7l1b*^{zf157tg} (Gribble et al., 2009) and *tcf7l2*^{zf55} (Muncan et al., 2007). These three lines are likely to abrogate expression of proteins coded by the reading frame starting in exon 1. There is an alternative downstream transcription start site in mouse *tcf7l2* (Vacik et al., 2011) and likely in other *tcf* genes too (unpublished observations). It is not known if transcripts from these alternative start sites have any functional roles in embryos carrying the mutations above. Genomic DNA was isolated by HotSHOT method (Suppl. Materials and methods) and *tcf7l1a*^{m881} and *tcf7l2*^{zf55} mutations were genotyped by KASP assays (K Biosciences, assay barcode 1145062619) using 1µl of genomic DNA for 8µl of reaction volume PCR as described by K Biosciences. Adult zebrafish organs were dissected as in Supp. Materials and methods. The sizes of eye profiles were quantified from lateral view images of PFA fixed embryos by delineating the eye using Adobe Photoshop CS5 magic wand tool and measuring the area of pixels included in the delineated region. The surface area was then transformed from px^2 to μm^2. Embryos were scored as eyeless when no retinal tissue was observed. Even though in the rescue experiments there was variability in the size of the eyes, for the sake of simplicity, all embryos with distinguishable eyes were scored as having eyes. This binary categorisation made the rescued versus not-rescued eye phenotype more straightforward to score and free of subjective interpretation.

RNA extraction, reverse transcription and PCR: Total RNA was extracted from live embryos and adult zebrafish using Trizol (Invitrogen) and homogenised by pestle crushing and vortexing. SuperscriptII (Invitrogen) was used for reverse transcription under manufacturers' instructions using oligo dT and 1µg of RNA for 20µg reaction volume. The following primers were used to

amplify fragments of *tcf7l2* cDNA: region exon4/5 (Set a-F TCAAAACAGCTCTTCGGATTCCGAG, Set a-R CTGTAGGTGATCAGAGGTGTGAG), region exon15 (Set b-F GATCTGAGCGCCCCAAAGA AGTG Set b-R CGGGGAGGGAGAAATCATGGA GG).

***tcf7l2* splice variant cloning, mRNA synthesis, embryo microinjection and morpholinos:** *tcf7l2* splice variant DNA was cloned in pCS2+ or pCS2+MT expression vectors for mRNA synthesis. mRNA for overexpression was synthesised using SP6 RNA mMessage mMachine transcription kit (Ambion). One to two cell stage embryos were co-injected with 10nl of 5pg of GFP mRNA and morpholinos or *in vitro* synthesised mRNA at the indicated concentrations. Only embryos with an even distribution of GFP fluorescence were used for experiments. Morpholino sequences:

mo^{tcf7l2ATG} (5'-CATTTTTCCCGAGGAGCGCTAATTT-3'). Embryos injected with this morpholino fail to produce Tcf7l2 protein (Fig. S5).

mo^{SPtcf7l2} (5'-GCCCCTGCAAGGCAAAGACGGACGT-3'). This splice-blocking morpholino leads to exon skipping to generate a Tcf7l2 protein lacking exon 5 derived amino acids (Fig. S5). *tcf7l1a*$^{-/-}$ embryos injected with mo^{SPtcf7l2} lack eyes, a phenotype not seen when the morpholino is injected into *tcf7l1a*$^{+/-}$ siblings. No equivalent genetic mutation that leads to loss of exon 5 of *tcf7l2* exists but the loss of eye phenotype is consistent with other conditions in which the overall level of TCF-mediated repression is reduced (Dorsky et al., 2003).

moC (5'- CTGAACAGGCGGCAGGCGATCCACA -3'). This morpholino is a sequence scrambled version of mo^{SPtcf7l2}used as an injection control.

mo^{tcf7l1b} (5'-CATGTTTAACGTTACGGGCTTGTCT-3'; Dorsky et al., 2002). *tcf7l1a*$^{m881/m881}$ embryos injected with mo^{tcf7l1b} phenocopy the loss of eye phenotype seen in *tcf7l1a*$^{m881/m881}$*/tcf7l1b*$^{zf157tg/zf157tg}$ double mutants (Young and Wilson, unpublished).

In situ hybridisation and probe synthesis: Digoxigenin (DIG) and fluorescein (FLU)-labelled RNA probes were synthesized using T7 or T3 RNA polymerases (Promega) according to manufacturers' instructions and supplied with DIG or FLU labelled UTP (Roche). Probes were detected with anti-

DIG-AP (1:5000, Roche) or anti-FLU-AP (1:10000, Roche) antibodies and NBT/BCIP (Roche) or INT/BCIP (Roche) substrates according to standard protocols (Thisse and Thisse, 2008).

Luciferase reporter experiments: The following reporters were used: cdx1-luc (Hecht and Stemmler, 2003), engrailed-luc (McGrew et al., 1999), cJun-luc (Nateri et al., 2005), lef1-luc (Hovanes et al., 2001), siamois-luc (Brannon et al., 1997), and TOPflash (Molenaar et al., 1996). HEK cells were transfected according to standard methods and using the conditions described in Supp. Materials and Methods.

Zebrafish protein extraction: Embryos were washed once with chilled Ringers solution, de-yolked by passing through a narrow Pasteur pipette, washed three times in chilled Ringers solution supplemented with PMF (300mM) and EDTA (0.1mM). Samples were briefly spun down, media removed, Laemlli buffer 1X was added at 10µl per embryo and incubated for 10min at 100ºC with occasional vigorous vortexing before chilling on ice. Samples were loaded in polyacrylamide gels or stored at -20ºC.

HEK cell transfection, immunohistochemistry and co-immunoprecipitation: HEK cells grown in 6cm dishes and transfected with 4µg of each DNA with lipofectamine 2000 (Invitrogen) for 6hrs according to manufacturers instructions.

For immunohistochemistry cells were fixed 48hrs after transfection in 4% paraformaldehyde in PBS for 20 min at room temperature, washed with PBS, and permeabilized in 0.2% Triton X-100 in PBS for 5 min at room temperature. The protocol was followed at standard conditions (Supp. Materials and Methods).

For immunoprecipitation, cells were grown for 24hrs after transfection and then proteins were extracted following standard conditions (Supp. Materials and Methods). The eluate from antibody beads (30µl) was loaded in 10% polyacrylamide gels and proteins were detected by Western blots (standard conditions) using anti-myc (1/20,000, SC-40, SCBT), anti-HA (1/10,000, 3F10, Roche) and anti β-catenin (1/8000, Sigma, C7207), to detect the co-immunoprecipitated proteins. Antibodies

used on Western blots in Fig. S4 are anti human Tcf7l2 (N-20, SCBT) and anti-gamma tubulin (T9026, Sigma) HRP coupled secondary antibodies (1/2,000, sigma) were used and blots were developed using an ECL kit (Promega).

Yeast two-hybrid assays: N-terminal deletions of the first 53 amino acids of *tcf7l2* splice variants were cloned in *pGBK* and full-length β-catenin and a C-terminal deletion (all the frame after amino acid 210) of *tle3b* (NM_131780) into *pGAD* (Clontech). Combinations of plasmids to test two-hybrid interactions were co-transformed in Y2Gold yeast strain (Suppl. Materials and Methods). Transformed yeast where plated on -Leu-Trp dropout selective media agar plates supplemented with X-gal. Positive blue colonies were streaked to an -Ade-His-Leu-Trp dropout selective media agar plates supplemented with Aureoblastidin A and X-gal (Clontech yeast two-hybrid manual).

Acknowledgments

We thank members of our lab, Florencia Cavodeassi, Mate Varga, Caro Courbis, Jorge Reino, Andrea Sanchez and Ricardo Jarpa for stimulating discussions, the UCL fish facility team for fish care and Elke Ober, Richard Dorsky, Marian Waterman, Randy Moon and others for reagents; Masa Kai for advice on Western blot methods and Abdol Nateri for advice on HEK cell protein extraction. This study was generously supported by the Wellcome Trust (S.W. and R.Y.), a Marie Curie Incoming International Fellowship (R.Y.), a Royal Society International Joint Project (S.W. and M.A.) and FONDAP (15090007) to (M.A).

Conflict of interest

The authors declare that they have no conflict of interest.

Author contributions: RMY and SWW conceived the study; RMY, KBE and VPF did experiments; RMY and SWW wrote the paper with input from all authors.

References

Arce L, Pate KT, Waterman ML (2009) Groucho binds two conserved regions of LEF-1 for HDAC-dependent repression. BMC Cancer 9: 159

Archbold HC, Yang YX, Chen L, Cadigan KM (2012) How do they do Wnt they do?: regulation of transcription by the Wnt/beta-catenin pathway. Acta Physiol (Oxf) 204: 74-109

Atcha FA, Munguia JE, Li TW, Hovanes K, Waterman ML (2003) A new beta-catenin-dependent activation domain in T cell factor. J Biol Chem 278: 16169-75

Atcha FA, Syed A, Wu B, Hoverter NP, Yokoyama NN, Ting JH, Munguia JE, Mangalam HJ, Marsh JL, Waterman ML (2007) A unique DNA binding domain converts T-cell factors into strong Wnt effectors. Mol Cell Biol 27: 8352-63

Bailey KA, Savic D, Zielinski M, Park SY, Wang LJ, Witkowski P, Brady M, Hara M, Bell GI, Nobrega MA (2015) Evidence of non-pancreatic beta cell-dependent roles of Tcf7l2 in the regulation of glucose metabolism in mice. Hum Mol Genet 24: 1646-54

Boj SF, van Es JH, Huch M, Li VS, Jose A, Hatzis P, Mokry M, Haegebarth A, van den Born M, Chambon P, Voshol P, Dor Y, Cuppen E, Fillat C, Clevers H (2012) Diabetes risk gene and Wnt effector Tcf7l2/TCF4 controls hepatic response to perinatal and adult metabolic demand. Cell 151: 1595-607

Brannon M, Brown JD, Bates R, Kimelman D, Moon RT (1999) XCtBP is a XTcf-3 co-repressor with roles throughout Xenopus development. Development 126: 3159-70

Brantjes H, Roose J, van De Wetering M, Clevers H (2001) All Tcf HMG box transcription factors interact with Groucho-related co-repressors. Nucleic Acids Res 29: 1410-9

Cadigan KM (2012) TCFs and Wnt/beta-catenin signaling: more than one way to throw the switch. Curr Top Dev Biol 98: 1-34

Cadigan KM, Waterman ML (2012) TCF/LEFs and Wnt signaling in the nucleus. Cold Spring Harb Perspect Biol 4

Cavallo RA, Cox RT, Moline MM, Roose J, Polevoy GA, Clevers H, Peifer M, Bejsovec A (1998) Drosophila Tcf and Groucho interact to repress Wingless signalling activity. Nature 395: 604-8

Chang MV, Chang JL, Gangopadhyay A, Shearer A, Cadigan KM (2008) Activation of wingless targets requires bipartite recognition of DNA by TCF. Curr Biol 18: 1877-81

Chodaparambil JV, Pate KT, Hepler MR, Tsai BP, Muthurajan UM, Luger K, Waterman ML, Weis WI (2014) Molecular functions of the TLE tetramerization domain in Wnt target gene repression. EMBO J 33: 719-31

Daniels DL, Weis WI (2005) Beta-catenin directly displaces Groucho/TLE repressors from Tcf/Lef in Wnt-mediated transcription activation. Nat Struct Mol Biol 12: 364-71

Davidson G, Wu W, Shen J, Bilic J, Fenger U, Stannek P, Glinka A, Niehrs C (2005) Casein kinase 1 gamma couples Wnt receptor activation to cytoplasmic signal transduction. Nature 438: 867-72

Dorsky RI, Itoh M, Moon RT, Chitnis A (2003) Two tcf3 genes cooperate to pattern the zebrafish brain. Development 130: 1937-47

Duval A, Rolland S, Tubacher E, Bui H, Thomas G, Hamelin R (2000) The human T-cell transcription factor-4 gene: structure, extensive characterization of alternative splicings, and mutational analysis in colorectal cancer cell lines. Cancer Res 60: 3872-9

Elfert S, Weise A, Bruser K, Biniossek ML, Jagle S, Senghaas N, Hecht A (2013) Acetylation of human TCF4 (TCF7L2) proteins attenuates inhibition by the HBP1 repressor and induces a conformational change in the TCF4::DNA complex. PLoS One 8: e61867

Ewan K, Pajak B, Stubbs M, Todd H, Barbeau O, Quevedo C, Botfield H, Young R, Ruddle R, Samuel L, Battersby A, Raynaud F, Allen N, Wilson S, Latinkic B, Workman P, McDonald E, Blagg J, Aherne W, Dale T (2010) A useful approach to identify novel small-molecule inhibitors of Wnt-dependent transcription. Cancer Res 70: 5963-73

Grant SF, Thorleifsson G, Reynisdottir I, Benediktsson R, Manolescu A, Sainz J, Helgason A, Stefansson H, Emilsson V, Helgadottir A, Styrkarsdottir U, Magnusson KP, Walters GB, Palsdottir E,

Jonsdottir T, Gudmundsdottir T, Gylfason A, Saemundsdottir J, Wilensky RL, Reilly MP et al. (2006) Variant of transcription factor 7-like 2 (TCF7L2) gene confers risk of type 2 diabetes. Nat Genet 38: 320-3

Gribble SL, Kim HS, Bonner J, Wang X, Dorsky RI (2009) Tcf3 inhibits spinal cord neurogenesis by regulating sox4a expression. Development 136: 781-9

Hallikas O, Taipale J (2006) High-throughput assay for determining specificity and affinity of protein-DNA binding interactions. Nat Protoc 1: 215-22

Hecht A, Stemmler MP (2003) Identification of a promoter-specific transcriptional activation domain at the C terminus of the Wnt effector protein T-cell factor 4. J Biol Chem 278: 3776-85

Heisenberg CP, Houart C, Take-Uchi M, Rauch GJ, Young N, Coutinho P, Masai I, Caneparo L, Concha ML, Geisler R, Dale TC, Wilson SW, Stemple DL (2001) A mutation in the Gsk3-binding domain of zebrafish Masterblind/Axin1 leads to a fate transformation of telencephalon and eyes to diencephalon. Genes Dev 15: 1427-34

Hikasa H, Ezan J, Itoh K, Li X, Klymkowsky MW, Sokol SY (2010) Regulation of TCF3 by Wnt-dependent phosphorylation during vertebrate axis specification. Dev Cell 19: 521-32

Hoppler, S. and Waterman, M. L. (2014) Evolutionary Diversification of Vertebrate TCF/LEF Structure, Function, and Regulation, in Wnt Signaling in Development and Disease: Molecular Mechanisms and Biological Functions (eds S. Hoppler and R. T. Moon), pp. 225-237. John Wiley & Sons, Inc, Hoboken, NJ, USA.

Houart C, Caneparo L, Heisenberg C, Barth K, Take-Uchi M, Wilson S (2002) Establishment of the telencephalon during gastrulation by local antagonism of Wnt signaling. Neuron 35: 255-65

Hovanes K, Li TW, Munguia JE, Truong T, Milovanovic T, Lawrence Marsh J, Holcombe RF, Waterman ML (2001) Beta-catenin-sensitive isoforms of lymphoid enhancer factor-1 are selectively expressed in colon cancer. Nat Genet 28: 53-7

Hoverter NP, Ting JH, Sundaresh S, Baldi P, Waterman ML (2012) A WNT/p21 circuit directed by the C-clamp, a sequence-specific DNA binding domain in TCFs. Mol Cell Biol 32: 3648-62

Hoverter NP, Zeller MD, McQuade MM, Garibaldi A, Busch A, Selwan EM, Hertel KJ, Baldi P, Waterman ML (2014) The TCF C-clamp DNA binding domain expands the Wnt transcriptome via alternative target recognition. Nucleic Acids Res 42: 13615-32

Hrckulak D, Kolar M, Strnad H, Korinek V (2016) TCF/LEF Transcription Factors: An Update from the Internet Resources. Cancers (Basel) 8

Hüsken U, Stickney HL, Gestri G, Bianco IH, Faro A, Young RM, Roussigne M, Hawkins TA, Beretta CA, Brinkmann I, Paolini A, Jacinto R, Albadri S, Dreosti E, Tsalavouta M, Schwarz Q, Cavodeassi F, Barth AK, Wen L, Zhang B et al. (2014) Tcf7l2 is required for left-right asymmetric differentiation of habenular neurons. Curr Biol 24: 2217-27

Kiecker C, Niehrs C (2001) A morphogen gradient of Wnt/beta-catenin signalling regulates anteroposterior neural patterning in Xenopus. Development 128: 4189-201

Kim CH, Oda T, Itoh M, Jiang D, Artinger KB, Chandrasekharappa SC, Driever W, Chitnis AB (2000) Repressor activity of Headless/Tcf3 is essential for vertebrate head formation. Nature 407: 913-6

Kimmel CB, Ballard WW, Kimmel SR, Ullmann B, Schilling TF (1995) Stages of embryonic development of the zebrafish. Dev Dyn 203: 253-310

Koga H, Tsedensodnom O, Tomimaru Y, Walker EJ, Lee HC, Kim KM, Yano H, Wands JR, Kim M (2012) Loss of the SxxSS motif in a human T-cell factor-4 isoform confers hypoxia resistance to liver cancer: an oncogenic switch in Wnt signaling. PLoS One 7: e39981

Korinek V, Barker N, Moerer P, van Donselaar E, Huls G, Peters PJ, Clevers H (1998) Depletion of epithelial stem-cell compartments in the small intestine of mice lacking Tcf-4. Nat Genet 19: 379-83

Li L, Mao J, Sun L, Liu W, Wu D (2002) Second cysteine-rich domain of Dickkopf-2 activates canonical Wnt signaling pathway via LRP-6 independently of dishevelled. J Biol Chem 277: 5977-81

Liu F, van den Broek O, Destree O, Hoppler S (2005) Distinct roles for Xenopus Tcf/Lef genes in mediating specific responses to Wnt/beta-catenin signalling in mesoderm development. Development 132: 5375-85

Lyssenko V, Lupi R, Marchetti P, Del Guerra S, Orho-Melander M, Almgren P, Sjogren M, Ling C, Eriksson KF, Lethagen AL, Mancarella R, Berglund G, Tuomi T, Nilsson P, Del Prato S, Groop L (2007) Mechanisms by which common variants in the TCF7L2 gene increase risk of type 2 diabetes. J Clin Invest 117: 2155-63

MacDonald BT, He X (2012) Frizzled and LRP5/6 receptors for Wnt/beta-catenin signaling. Cold Spring Harb Perspect Biol 4

MacDonald BT, Tamai K, He X (2009) Wnt/beta-catenin signaling: components, mechanisms, and diseases. Dev Cell 17: 9-26

Mahmoudi T, Li VS, Ng SS, Taouatas N, Vries RG, Mohammed S, Heck AJ, Clevers H (2009) The kinase TNIK is an essential activator of Wnt target genes. EMBO J 28: 3329-40

McGrew LL, Takemaru K, Bates R, Moon RT (1999) Direct regulation of the Xenopus engrailed-2 promoter by the Wnt signaling pathway, and a molecular screen for Wnt-responsive genes, confirm a role for Wnt signaling during neural patterning in Xenopus. Mech Dev 87: 21-32

Molenaar M, van de Wetering M, Oosterwegel M, Peterson-Maduro J, Godsave S, Korinek V, Roose J, Destree O, Clevers H (1996) XTcf-3 transcription factor mediates beta-catenin-induced axis formation in Xenopus embryos. Cell 86: 391-9

Morita T, Nitta H, Kiyama Y, Mori H, Mishina M (1995) Differential expression of two zebrafish emx homeoprotein mRNAs in the developing brain. Neurosci Lett 198: 131-4

Muncan V, Faro A, Haramis AP, Hurlstone AF, Wienholds E, van Es J, Korving J, Begthel H, Zivkovic D, Clevers H (2007) T-cell factor 4 (Tcf7l2) maintains proliferative compartments in zebrafish intestine. EMBO Rep 8: 966-73

Nateri AS, Spencer-Dene B, Behrens A (2005) Interaction of phosphorylated c-Jun with TCF4 regulates intestinal cancer development. Nature 437: 281-5

Nguyen H, Merrill BJ, Polak L, Nikolova M, Rendl M, Shaver TM, Pasolli HA, Fuchs E (2009) Tcf3 and Tcf4 are essential for long-term homeostasis of skin epithelia. Nat Genet 41: 1068-75

Niehrs C (2012) The complex world of WNT receptor signalling. Nat Rev Mol Cell Biol 13: 767-79

Nusse R, Clevers H (2017) Wnt/beta-Catenin Signaling, Disease, and Emerging Therapeutic Modalities. Cell 169: 985-999

Ota S, Ishitani S, Shimizu N, Matsumoto K, Itoh M, Ishitani T (2012) NLK positively regulates Wnt/beta-catenin signalling by phosphorylating LEF1 in neural progenitor cells. EMBO J 31: 1904-15

Prokunina-Olsson L, Welch C, Hansson O, Adhikari N, Scott LJ, Usher N, Tong M, Sprau A, Swift A, Bonnycastle LL, Erdos MR, He Z, Saxena R, Harmon B, Kotova O, Hoffman EP, Altshuler D, Groop L, Boehnke M, Collins FS et al. (2009) Tissue-specific alternative splicing of TCF7L2. Hum Mol Genet 18: 3795-804

Pukrop T, Gradl D, Henningfeld KA, Knochel W, Wedlich D, Kuhl M (2001) Identification of two regulatory elements within the high mobility group box transcription factor XTCF-4. J Biol Chem 276: 8968-78

Roose J, Molenaar M, Peterson J, Hurenkamp J, Brantjes H, Moerer P, van de Wetering M, Destree O, Clevers H (1998) The Xenopus Wnt effector XTcf-3 interacts with Groucho-related transcriptional repressors. Nature 395: 608-12

Savic D, Ye H, Aneas I, Park SY, Bell GI, Nobrega MA (2011) Alterations in TCF7L2 expression define its role as a key regulator of glucose metabolism. Genome Res 21: 1417-25

Schuijers J, Mokry M, Hatzis P, Cuppen E, Clevers H (2014) Wnt-induced transcriptional activation is exclusively mediated by TCF/LEF. EMBO J 33: 146-56

Shetty P, Lo MC, Robertson SM, Lin R (2005) C. elegans TCF protein, POP-1, converts from repressor to activator as a result of Wnt-induced lowering of nuclear levels. Dev Biol 285: 584-92

Sokol SY (2011) Wnt signaling through T-cell factor phosphorylation. Cell Res 21: 1002-12

Thisse C, Thisse B (2008) High-resolution in situ hybridization to whole-mount zebrafish embryos. Nat Protoc 3: 59-69

Tsedensodnom O, Koga H, Rosenberg SA, Nambotin SB, Carroll JJ, Wands JR, Kim M (2011) Identification of T-cell factor-4 isoforms that contribute to the malignant phenotype of hepatocellular carcinoma cells. Exp Cell Res 317: 920-31

Vacik T, Stubbs JL, Lemke G (2011) A novel mechanism for the transcriptional regulation of Wnt signaling in development. Genes Dev 25: 1783-95

Valenta T, Lukas J, Korinek V (2003) HMG box transcription factor TCF-4's interaction with CtBP1 controls the expression of the Wnt target Axin2/Conductin in human embryonic kidney cells. Nucleic Acids Res 31: 2369-80

van Amerongen R, Nusse R (2009) Towards an integrated view of Wnt signaling in development. Development 136: 3205-14

van Beest M, Dooijes D, van De Wetering M, Kjaerulff S, Bonvin A, Nielsen O, Clevers H (2000) Sequence-specific high mobility group box factors recognize 10-12-base pair minor groove motifs. J Biol Chem 275: 27266-73

van de Wetering M, Cavallo R, Dooijes D, van Beest M, van Es J, Loureiro J, Ypma A, Hursh D, Jones T, Bejsovec A, Peifer M, Mortin M, Clevers H (1997) Armadillo coactivates transcription driven by the product of the Drosophila segment polarity gene dTCF. Cell 88: 789-99

Weise A, Bruser K, Elfert S, Wallmen B, Wittel Y, Wohrle S, Hecht A (2010) Alternative splicing of Tcf7l2 transcripts generates protein variants with differential promoter-binding and transcriptional activation properties at Wnt/beta-catenin targets. Nucleic Acids Res 38: 1964-81

Wilson SW, Houart C (2004) Early steps in the development of the forebrain. Dev Cell 6: 167-81

Wohrle S, Wallmen B, Hecht A (2007) Differential control of Wnt target genes involves epigenetic mechanisms and selective promoter occupancy by T-cell factors. Mol Cell Biol 27: 8164-77

Xue Y, Ren J, Gao X, Jin C, Wen L, Yao X (2008) GPS 2.0, a tool to predict kinase-specific phosphorylation sites in hierarchy. Mol Cell Proteomics 7: 1598-608

Yamamoto H, Ihara M, Matsuura Y, Kikuchi A (2003) Sumoylation is involved in beta-catenin-dependent activation of Tcf-4. EMBO J 22: 2047-59

Young RM, Reyes AE, Allende ML (2002) Expression and splice variant analysis of the zebrafish tcf4 transcription factor. Mech Dev 117: 269-73

Zeng X, Tamai K, Doble B, Li S, Huang H, Habas R, Okamura H, Woodgett J, He X (2005) A dual-kinase mechanism for Wnt co-receptor phosphorylation and activation. Nature 438: 873-7

Figure Legends

Fig. 1. Description and expression of a new alternatively spliced exon in zebrafish *tcf7l2*.

(**A**) Schematic representation of variants of Tcf7l2 arising from different splice forms (not to scale). Labels 4 and 5 represent the region of Tcf7l2 coded by alternative exons 4 and 5. Short (S), Medium (M) and Long (L) C-terminal variants coded by alternative splice variants in the 5' end of exon 15 are indicated. Red box, β-catenin (βcat) binding domain. Green boxes, High-Mobility Group (HMG) Box, which is the primary DNA interacting domain, and C-clamp DNA-helper binding domain. Yellow boxes, CtBP interaction domains. CDRD labelled line over exons 4 and 5 indicates the Context Dependent Regulatory Domain and GBS (Groucho Binding Site) marks the region of interaction with Groucho/Tle transcriptional co-repressors. Arrows indicate the position of primer sets 'a' and 'b' used for RT-PCR experiments in (E).

(**B-C**) Alignment of the amino acid sequences coded by zebrafish, *Takifugu rubripens* and *Tetradon tcf7l2* exon 5 (B) or human exon 3a (C). Identical amino acids marked by blue boxes. Asterisks over sequence mark putative phosphorylated amino acids. Dots over sequence indicate similar amino acids.

(D) Schematic of the genomic region of zebrafish and human *tcf7l2*. Introns depicted as lines and exons as boxes. Blue exon boxes depict human *tcf7l2* alternative exons 3a and 4a, and zebrafish alternative exon 5. Black exon boxes indicate equivalent exons in both species emphasised by arrows. Numbers under introns and within exons represent their nucleotide size (not to scale).

(**E**) RT-PCR experiments performed on cDNA from embryos of ages indicated in hours post fertilisation (hpf). L, 1Kb ladder. Top panel shows results of PCRs using primer set 'a' (materials and methods) amplifying the region of alternative exons 4 and 5. Bottom panel shows results of PCRs using primer set 'b' (materials and methods) amplifying the region of alternative exon 15. Asterisk shows maternal expression of *tcf7l2*.

(**F-G**) Double *in situ* hybridisation of *tcf7l2*, in blue, and *emx3* (F) or *pax2a* (G), in red. 10hpf flat mounted embryos, dorsal view, anterior up, posterior down; fb, prospective forebrain; mb, prospective midbrain. Scale Bar in (F) is 200µm.

Fig. 2. Alternative exon 5 of *tcf7l2* impacts eye formation.

(A-F) Lateral views (anterior to left, dorsal up) of 28hpf live wildtype (A), *tcf7l2*$^{zf55/zf55}$ (B), double *tcf7l1a*$^{-/-}$/*tcf7l2*$^{zf55/zf55}$ (C) and *tcf7l1a*$^{-/-}$ (D-F) zebrafish embryos with injected reagents indicated top right showing representative phenotypes. (D) 0.12pmol mo^{tcf7l1b} (E), 0.12pmol mo^{tcf7l1b} and 20pg of *45L-tcf72* splice variant mRNA, (F) 1.25pmol mo^{SPtcf7l2}. Scale bar in (A) is 200µm.

(**G**) Plot showing the area of the profile of eyes of 30hpf fixed embryos coming from a double heterozygous *tcf7l1a/tcf7l2* mutant incross. Error bars are mean ±SD, P values from unpaired t test with Welch's correction comparing wildtype and the stated genetic combinations. Percentages indicate average eye profile size relative to wildtype.

(**H**) Bars represent the percentage of *tcf7l1a*$^{-/-}$ embryos that develop eyes (with distinguishable lens and pigmented retina) coming from multiple *tcf7l1a*$^{+/-}$ female to *tcf7l1a*$^{-/-}$ males crosses, injected with 0.12pmol of mo^{tcf7l1b} (all bars) and co-injected with constructs stated on X axis: 10pg of *tcf7l1a* mRNA (A), 20pg of *tcf7l2* mRNA splice variants *4L-tcf7l2* (B), *45L-tcf7l2*, (C), *myc-4L-tcf7l2* (D), *myc-45L-tcf7l2* (E), *tcf7l2*-AA (F). Data for all these plots is included in TableS4. Error bars are mean ±SD.

Fig. 3. Alternative exon 5 of *tcf7l2* facilitates suppression of transcription mediated by constitutively active *VP16-TCF7L2*.

Bar plots showing luciferase reporter assay results expressed in relative light units. HEK293 cells were transiently co-transfected with luciferase reporter constructs indicated beneath X-axis, *VP16-TCF7L2* DNA (apart from first bars) and *4L-tcf7l2* DNA (+4L; 3rd bars), or *45L-tcf7l2* DNA (+45L; 4th bars) or *tcf7l2-AA* DNA (+AA; 5th bars). Control experiments show only background luciferase activity with no transfected plasmids (1st bars). Figures in the bars indicate the percentage size of that bar relative to transfection with *VP16-TCF7L2* alone (2nd bar). Error bars are mean ±SD n=3, P values from unpaired t tests with Welch's correction comparing *VP16-TCF7L2* control condition with *tcf7l2* variant co-transfections. Comparisons with no statistical significance are not marked.

Fig. 4. Alternative exon 5 of *tcf7l2* enhances affinity with Tle3b

Protein input (left panel) and anti-Myc immunoprecipitation (IP) eluate western blot (right panel) showing co-inmunoprecipitation of β-Catenin or HA-tagged Tle3b. HEK293 cells were transiently transfected with HA tagged *tle3b* together with empty myc tag vector (1st lane), myc-*4L-tcf7l2* (2nd lane), *myc-45-tcf7l2* (3rd lane) and *myc-AA-tcf7l2* (4th lane). Left panels show protein input before anti-Myc IP. Right panels show protein eluate from anti-Myc antibody coupled beads. Westernblots were probed with anti-Myc (tagged Tcf7l2 proteins, top panel), anti-βcatenin (middle panel) and anti-HA (tagged Tle3b protein, bottom panel) antibodies. Asterisk shows that the Tcf7l2 form containing exon 5 shows more intense binding with Tle3b than other Tcf7l2 forms.

Young_Fig1

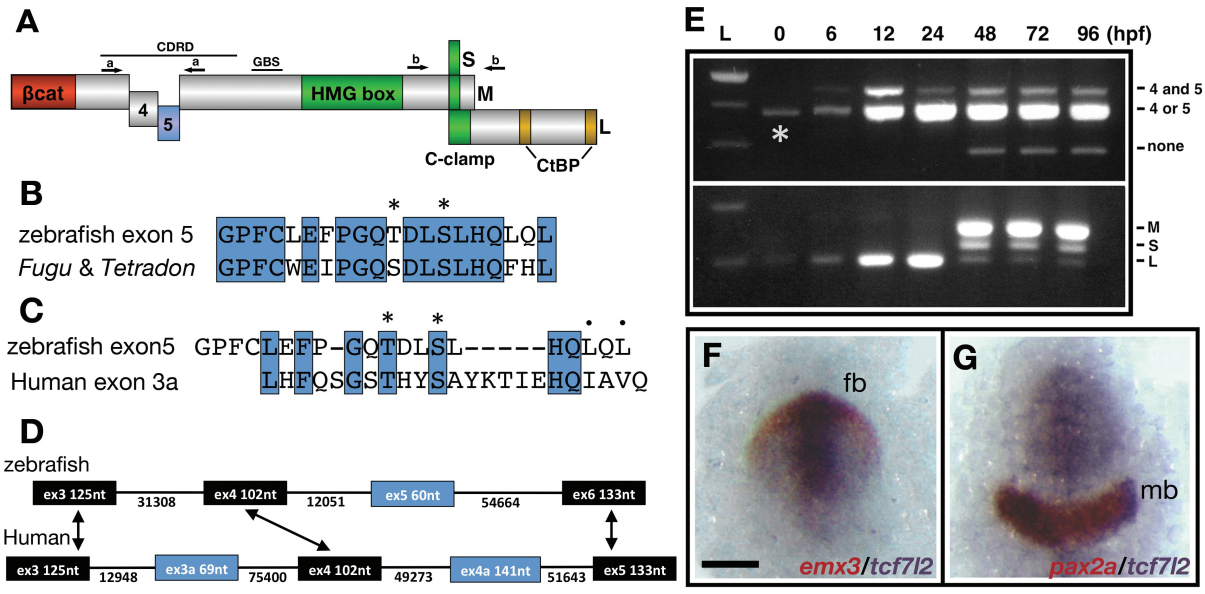

Young_Fig2

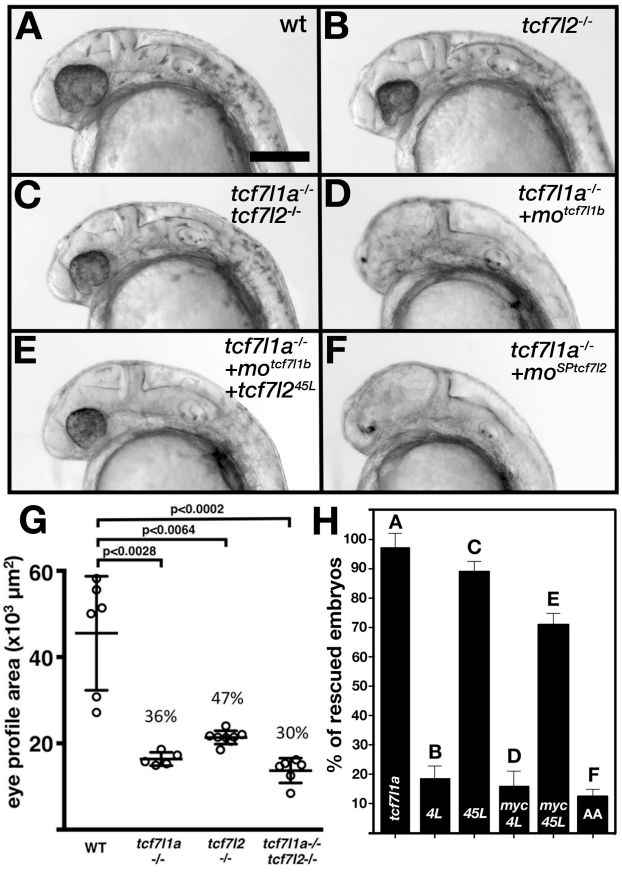

Young_Fig3

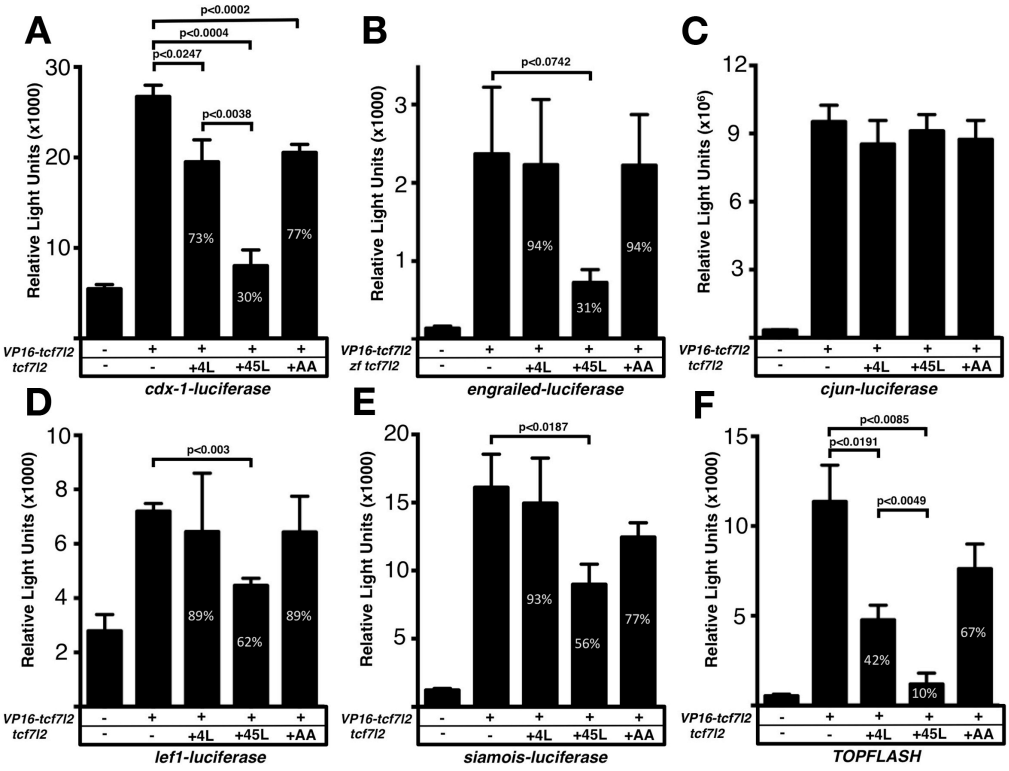

Young_Fig4

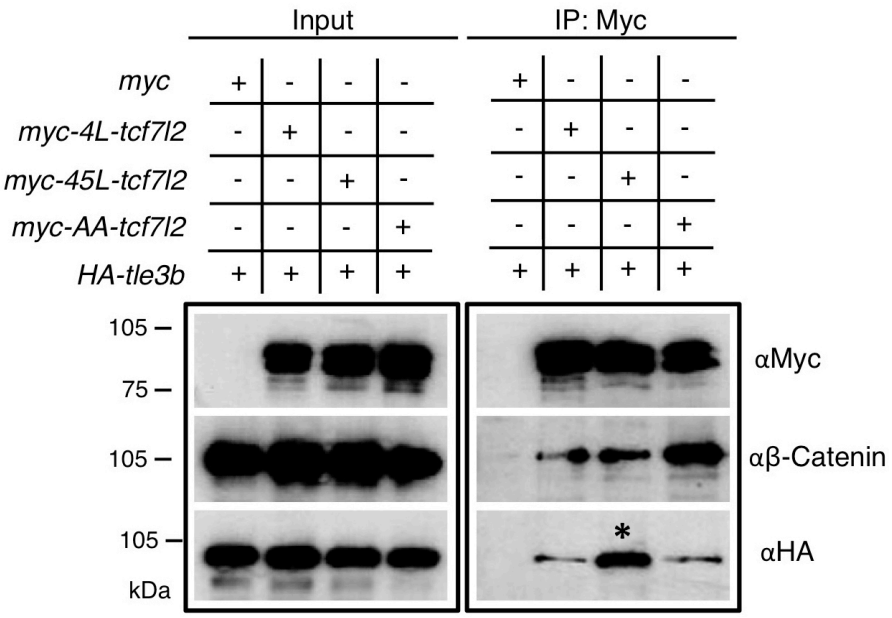

A

		0	6	12	24	48	72	96	(hpf)
	only exon 4	+	+	++	++	+	+	+	
	only exon 5	-	-	-	-	+	+	+	
	no exon4/5	-	-	-	-	+	+	+	
	exons 4&5	-	+	+	+	+	+	+	
exon 4 vs exon15	Short-Ct	-	-	-	-	+	+	+	
exon 4 vs exon15	Medium-Ct	-	-	-	-	++	++	++	
exon 4 vs exon15	Long-Ct	+	+	+	+	+	+	+	
exon 5 vs exon15	Short-Ct	-	-	-	-	+	+	-	
exon 5 vs exon15	Medium-Ct	-	-	-	-	++	++	++	
exon 5 vs exon15	Long-Ct	-	+	+	+	-	-	-	

B

Tcf7l2 variant	0	6	12	24	48	72	96	(hpf)
4S	-	-	-	-	+	+	+	
4M	-	-	-	-	+	+	+	
4L	+	+	+	+	+	+	+	
5S	-	-	-	-	+	+	-	
5M	-	-	-	-	+	+	+	
5L	-	-	-	-	-	-	-	
45S	-	-	-	-	?	?	-	
45M	-	-	-	-	?	?	?	
45L	-	+	+	+	-	-	-	

Table S1 Summary table of RT-PCR analyses showing developmental expression of alternative *tcf7l2* exons 4, 5 and 15 (A) and Tcf7l2 variants (B) through development.

(**A**) Results in rows 1 to 4 (grey) taken from Fig1E, rows 5 to 7 (pink) from FigS3A and rows 8 to 10 (blue) from FigS3B. (+) and (++) depict relative band intensity in the gels; (-) indicates no signal

(**B**) Tcf7l2 variants expressed during development based on the information in (A). (+) and (-) indicate presence or absence of the variant respectively. (?) indicates that it is not possible to derive a conclusion based on the data available. Analysis of variants that lack both exons 4 and 5 is not included.

A

		Eye	Brain	Gut	Liver	Pancras	Ovaries	Testes
	exon 4	++	++	++	++	++	++	++
	exon 5	-	+	-	-	-	-	-
	no exon4/5	-	+	-	-	-	-	-
	exons 4&5	+	+	+	+	+	+	+
exon 4 vs exon15	Short-Ct	+	++	-	-	-	-	-
	Medium-Ct	-	+	-	-	+	-	-
	Long-Ct	+	-	+	+	-	+	+
exon 5 vs exon15	Short-Ct	-	++	-	-	-	-	-
	Medium-Ct	+	+	-	-	+	-	-
	Long-Ct	++	-	+	+	++	+	+

B

Tcf7l2 variant	Eye	Brain	Gut	Liver	Pancras	Ovaries	Testes
4S	+	?	-	-	-	-	-
4M	-	?	-	-	+	-	-
4L	+	-	+	+	-	+	+
5S	-	?	-	-	-	-	-
5M	+	?	-	-	-	-	-
5L	+	-	-	-	-	-	-
45S	-	?	-	-	-	-	-
45M	-	?	-	-	+	-	-
45L	+	-	+	+	+	+	+

Table S2 Summary table of RT-PCR analysis of alternative *tcf7l2* exons 4, 5 and 15 (A) and Tcf7l2 variants (B) expressed in adult organs.

(**A**) Results in rows 1 to 4 (grey) taken from FigS3C, rows 5 to 7 (pink) from FigS3E and rows 8 to 10 (blue) from FigS3F. (+) and (++) depict relative band intensity in the gels; (-) indicates no signal

(**B**) Tcf7l2 variants expressed in adult organs based on the information in (A). (+) and (-) indicate presence or absence of the variant respectively. (?) indicates that it is not possible to derive a conclusion based on the data. Analysis of variants that lack both exons 4 and 5 is not included.

	%eyeless	%with eyes	total
0.12pmol mo *tcf7l1b*	52	48	95
	49	51	216
	49	51	228
1.25pmol moSP *tcf7l2*	49	51	126
	52	48	58
	49	51	70

Table S3 Knockdown of *tcf7l1b* and excision of *tcf7l2* exon5 in *tcf7l1a*$^{-/-}$ mutant embryo compromises eye formation

Embryos from female *tcf7l1a*$^{+/-}$ to male *tcf7l1a*$^{-/-}$ spawnings were injected with the morpholinos stated in the left column. This pairing scheme leads to 50% of homozygous mutant embryos. Each row represents an individual experiment. Embryos were scored as eyeless when little or no pigmented retinal tissue could be distinguished. Total represents the number of embryos scored in each experiment.

mRNA injected	%eyeless	%with eyes	%rescue	total
tcf7l1a	4	96	91	140
	0	100	100	73
	0	100	100	69
4L-tcf7l2	41	59	17	111
	43	57	15	108
	38	62	23	73
45L-tcf7l2	4	96	93	139
	7	93	86	100
	6	94	89	87
myc-4L-tcf7l2	44	56	11	45
	42	58	15	113
	39	61	21	140
myc-45L-tcf7l2	13	87	73	180
	17	83	66	149
	13	87	73	67
AA-tcf7l2	42	58	15	113
	45	55	10	69
	44	56	12	50

Table S4. Restoration of eye formation by expression of exogenous Tcf7l2 variants in *tcf7l1a*$^{-/-}$ */tcf7l1b* morphant embryos.

Embryos from female *tcf7l1a*$^{+/-}$ to male *tcf7l1a*$^{-/-}$ spawnings were co-injected with *tcf7l1b* morpholino and the *tcf7l2* mRNAs stated in the left column. In absence of exogenous Tcf7l2 this pairing scheme leads to 50% of eyeless offspring (Table S3). Each row represents an individual experiment. Total represents the number of embryos scored in each experiment. Eye formation was scored as rescued when pigmented retinal tissue was evident.

	wildtype	*tcf7l1a*$^{-/-}$	*tcf7l2*$^{-/-}$	*tcf7l1a*$^{-/-}$ *tcf7l2*$^{-/-}$
	55594	15289	21313	12509
	51380	15770	21717	14655
	50064	14911	18510	16180
	58204	17256	21457	8399
	27149	18603	22043	14989
	30765		21428	15352
			24022	
			20482	
Average	45526	16366	21371	13681
SD	13210	1535	1285	2862

Table S5 Size of the eye profile area is smaller in *tcf7l1a*$^{-/-}$ *and tcf7l2*$^{-/-}$ embryos at 30hpf.

Area in µm^2 of the eye profile of 30hpf fixed embryos coming from a double heterozygous *tcf7l1a/tcf7l2* mutant incross. SD, Standard Deviation.

A Nucleotide Sequence

TATCTACAGATGAAATGGCCCCTGCTAGATGTTCAAGCAGGAAGTCTTCAGAGTAGACAAGCACTTAAAGATGCCAGGTC
ACCTTCTCCAGCACACATCGTTGGGCCCTTCTGCTTGGAATTCCCCGGACAGACTGATCTGAGTCTTCACCAATTACAGT
TGTCTAATAAGGTCCCCGTGGTACAGCACCCTCACCATGTGCACCCGCTCACACCTCTGATCACCTACAGCAATGAGCAC
TTCACGCCTGGGAACCCCCCTCCACATCTACAGGCAGACGTGGACCCCAAAACAG

B Amino acid sequence

YLQMKWPLLDVQAGSLQSRQALKDARSPSPAHIVGPFCLEFPGQTDLSLHQLQLSNKVPVVQHPHHVHPLTPLITYSNEH
FTPGNPPPHLQGDVDPKT

Fig. S1. Zebrafish exon 5 nucleotide and coded amino acid sequences.

(A) Nucleotide sequence of zebrafish *tcf7l2* exon 5 (highlighted) and neighbouring exons.

(B) Amino acid sequence of the translated sequence of exons in (A).

A

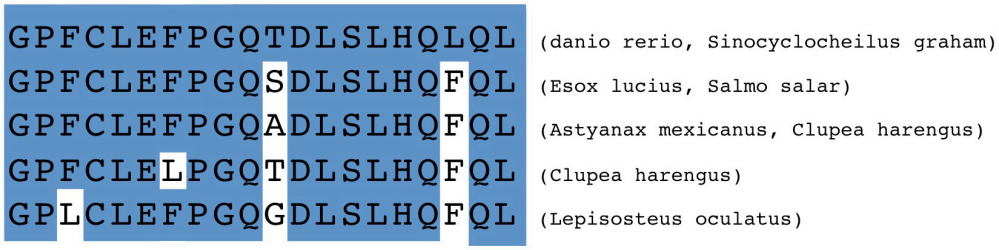

B

	ex3	Hs-ex5/Dr-ex4	ex6
nt	82%	82%	85%
aa	98%	100%	98%

Fig. S2. Alignment of the amino acid sequence coded by *tcf7l2* exon 5 in zebrafish and other fish species.

(**A**) Alignment of the zebrafish and other fish species amino acid sequence coded by *tcf7l2* exon 5.

(**B**) Table showing the nucleotide (nt) homology between human and zebrafish exons surrounding zebrafish new exon 5 and the amino acid (aa) identity of the protein regions they code. Hs, *Homo sapiens*; Dr, *Danio rerio*.

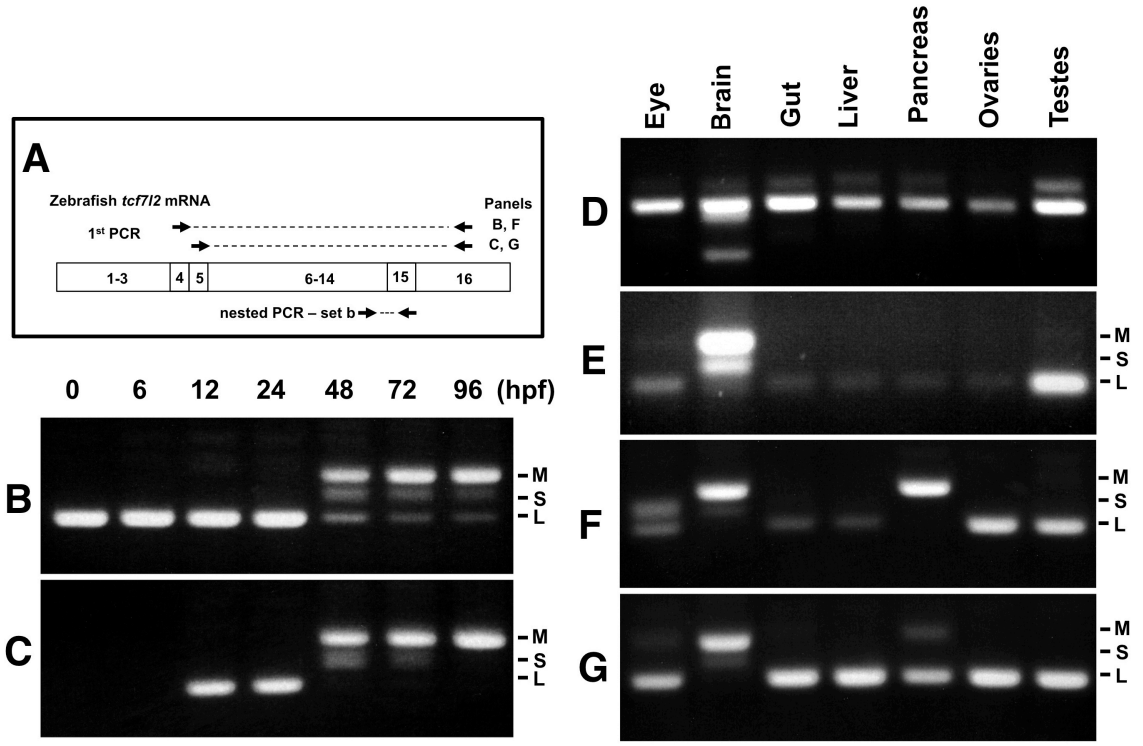

Fig. S3. Expression of *tcf7l2* alternative exons 4, 5 and 15 varies across development and in adult organs.

RT-PCR analyses of exons 4, 5 and 15 alternative borders of zebrafish *tcf7l2* across development and in various adult organs.

(**A**) Schematic representation of nested RT-PCR strategy used for panels (B, C, F and G).

(**B-C**) cDNA from embryos of ages indicated (hpf) was PCR amplified using a forward primer that anneals over exon 4 (**B**) or exon 5 (**C**) and a reverse primer that anneals to exon 16 common to all *tcf7l2* mRNA variants. The product from this first PCR was then used as a template for a nested PCR using primer set 'b' (as in Fig. 1.A) that amplifies exon 15 and reveals the different Ct ends of Tcf7l2. This last PCR product is shown in these panels. M (Medium), S (short) and L (Long) Ct Tcf7l2 variants.

(**D-E**) RT-PCR experiments performed on cDNA of the indicated adult organs using primer set 'a' (materials and methods) amplifying the region of alternative exons 4 and 5 (**D**) or using primer set 'b' (materials and methods) amplifying the region of alternative exon 15 (**E**).

(**F-G**) Same PCR amplification strategy used in panels (**B-C**) to detect the Ct *tcf7l2* variants associated with exons 4 or 5, but using the indicated adult organ cDNA as template in the 1st PCR reaction.

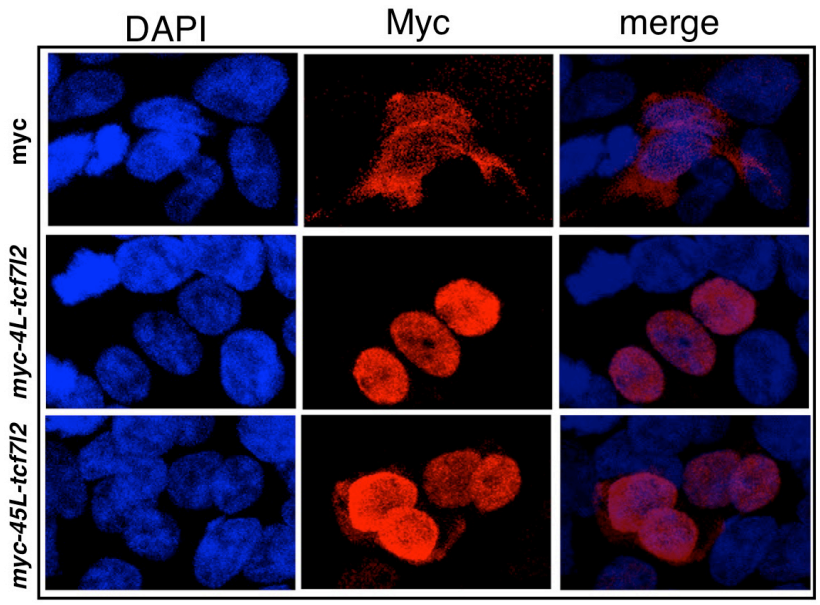

Fig. S4. Tcf7l2 variants localise to the nucleus.

Sub-cellular localisation of 4L-Tcf7l2 and 45L-Tcf7l2 myc tagged splice variants. HEK293 cells were transfected with empty myc tag vector (top row), *myc-4L-tcf7l2* (middle row) and *myc-45L-tcf7l2* (right row) splice variants and immunostained with anti-myc antibody (2nd column) and stained with DAPI (1st column). Merged images in 3rd column.

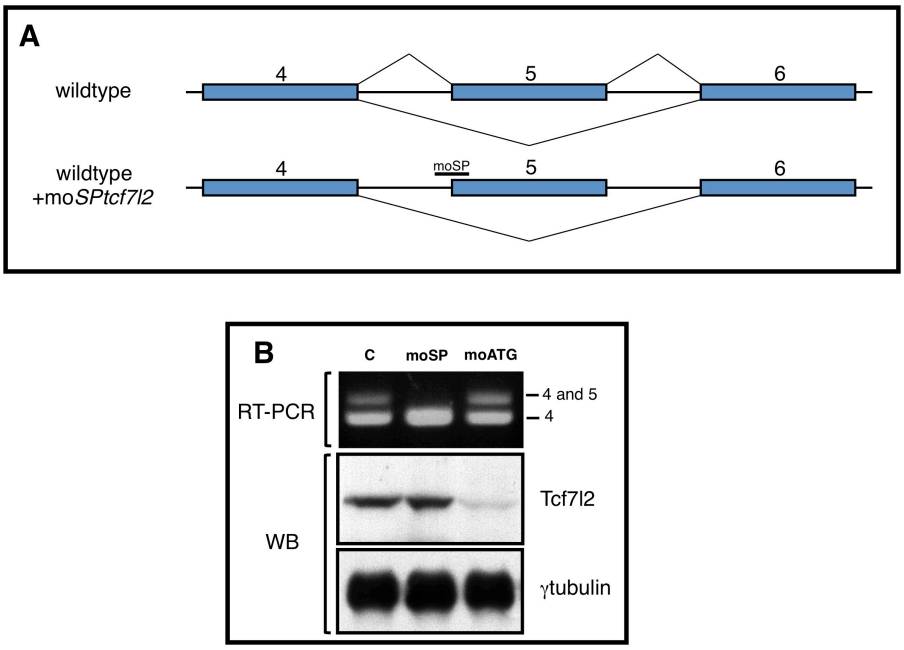

Fig. S5. Splicing specific morpholino knockdown of *tcf7l2* splice variants that include exon5.

(**A**) Cartoon showing the rationale of using mo^{SPtcf7l2} that targets intron 4/exon 5 splice site boundary blocking the splicing machinery and making it skip to the next splicing acceptor site in exon 6.

(**B**) RT-PCR (**top panel**) and Western blot (**middle and bottom panels**) performed using RNA and proteins extracted from 24hpf zebrafish embryos injected with: control morpholino (first lane), mo^{SPtcf7l2} (moSP, second lane), and mo^{ATGtcf7l2} (moATG, third lane). cDNA was amplified using set 'a' primers (Fig.1A, 5'F1 vs Splice R1, materials and methods). Anti human Tcf7l2 and anti-gamma tubulin antibodies were used in Western blot experiments (middle and bottom panel).

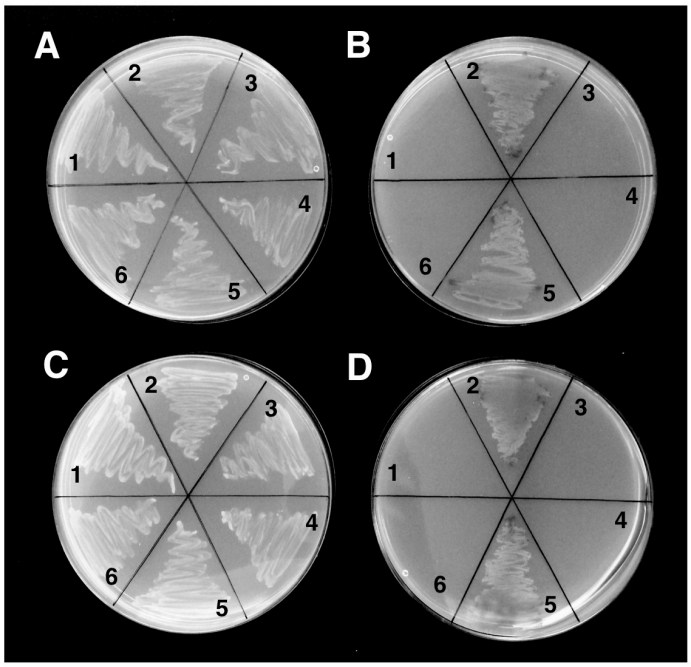

Fig. S6. 4L-Tcf7l2 and 45L-Tcf7l2 variants interact with β-Catenin and Tle3b in yeast two-hybrid protein interaction assays.

Y2Gold yeast strain was co-transformed with:

(**1**) β-catenin/*pGAD* and empty *pGBK* vector,

(**2**) β-catenin/*pGAD* and *4L-tcf7l2/pGBK* (**A, B**) or *45L-tcf7l2/pGBK* (**C, D**),

(**3**) empty *pGAD* vector and *4L-tcf7l2/pGBK* (**A, B**) or *45L-tcf7l2/pGBK* (**C, D**) with,

(**4**) *dCtle3b/pGAD* and Empty *pGBK* vector,

(**5**) *dCtle3b*/*pGAD* and *4L-tcf7l2/pGBK* (**A, B**) or *45L-tcf7l2/pGBK* (**C, D**),

(**6**) empty *pGBK* and *pGAD* vectors.

and plated in -Leu-Trp dropout selective media agar plates supplemented with Xgal (**A, C**) or

-Ade-His-Leu-Trp dropout selective media agar plates supplemented with Aureoblastidin A and X-gal (**B, D**).

Supplementary Materials and Methods

Genotyping and adult tissue dissection: Genomic DNA was extracted from methanol or 4% paraformaldehyde fixed embryos by incubating in 25µl of KOH 1.25M, EDTA 10mM at 95ºC for 30min, and then neutralised with 25µl of Tris-HCl 2M.

For tissue dissection, adult fish around a year old were culled by deep anesthetising in ice-cold 0.15% 2-phenotyethanol. Liver and pancreas tissue were isolated under a dissecting fluorescence microscope using *Tg*(*fabp10:dsRed*)^{gz4} (Dong et al., 2007) and *Tg*(*XlEef1a1:GFP*)^{s854} (Field et al., 2003) lines to distinguish liver and pancreas respectively. Other organs had clear anatomical boundaries and were easily dissected.

Luciferase Reporter HEK cell transformation and assay conditions: HEK293 cells were grown routinely in DMEM + 10% foetal bovine serum and penicillin/streptomycin (all Gibco from Thermo-Fisher/Invitrogen). White-sided, clear-bottomed 96 well plates (Corning) were seeded at 8,000 cells/well in 100µl/well medium without antibiotics. All transfections were carried out with Transfectin (Bio-Rad) at a ratio of 3/1 (0.3 µl Transfectin/100ng DNA). Competition assays were carried out using VP16-TCF4 as the constitutive TCF (Ewan et al., 2010). The following plasmid amounts were used: VP16-TCF4: 43.5 ng/well; 25 ng/well reporter plasmids; 25 ng/well TCF isoform +pcDNA; 6.5 ng/well pcDNA-lacZ totalling 100 ng/well DNA. Transfectin was pipetted into 12.5 µl/well OptiMEM (Gibco/Thermo-Fisher) and the appropriate amount of DNA (above) into another 12.5 µl/well OptiMEM. The two were mixed and complexes were allowed to form over 20 min. The complexes were applied to the cells for 4 hrs after which the medium was removed and replaced with a fresh 100 µl/well medium. After 2 days incubation, the medium was removed the cells were lysed in 50 µl/well GLO Lysis buffer (Promega) over 20 min on slow shake. The lysate was then split into two 25 µl/well fractions. The luciferase assay was carried out with 25 µl/well Bright-GLO (Promega) and the lacZ transfection control assay with 25 µl/well Beta-GLO (Promega). All measurements were taken on a Fluostar plate reader (BMG) set to luminescence mode.

HEK293 cell immunohistochemistry and co-immunoprecipitation protocol: For immuno-histochemistry, following cell fixation and permeabilisation, samples were washed with PBS, blocked in 5% albumin, and then incubated at 4°C overnight in mouse anti-MYC antibody high-affinity 9E10 (SCBT) diluted 1:1000 in 1% albumin in PBS. Cells were washed with PBS and incubated at room temperature for 1 h in Alexa Fluor 568 goat anti-mouse (Molecular Probes, Eugene, OR) diluted 1:1,000 in 1% albumin in PBS. Samples were washed with PBS, incubated in DAPI (1:50,000) for 5 min at room temperature, washed again, and mounted.

For Co-IP, following transformation, 350µl of Lysis Buffer 1 (below) was added and cells were resuspended off the plate by pipetting and lysed on ice for 1hr gently mixing every 10min. Samples were then centrifuged at 16.000g for 15min at 4ºC, to enable removal of the supernatant and samples were then stored on ice. 70µl of Lysis Buffer 2 was added to the pellet which was then sonicated three times for 5 seconds each. Tubes were centrifuged at 16.000g for 15min at 4ºC and the supernatant was collected and added to the supernatant of the previous centrifugation step. Proteins were quantified by BCA method (Sigma, BCA1).

Lysis Buffer 1: NaCl 150mM, Tris-HCl 80mM pH7.2, NP-40 0.5%, Glycerol 20%. 10µl of complete protease Inhibitor (Sigma, P-8340), 10µl of phosphatase Inhibitor 1 (Sigma, P-2850) and 10µl of phosphatase Inhibitor 2 (Sigma, P-5726) were added before protein extraction for each 1ml of lysis buffer.

Lysis Buffer 2: NaCl 300mM, Tris-HCl 20mM pH7.2, SDS 0.01%, Triton 1%, EDTA 2mM, add 10µl of complete protease Inhibitor (Sigma, P-8340), 10µl of phosphatase Inhibitor 1 (Sigma, P-2850) and 10µl of phosphatase Inhibitor 2 (Sigma, P-5726) were added before protein extraction for each 1ml of lysis buffer.

For each Immunoprecipitation (IP) experiment condition 40µl of anti-myc bead slurry (Sigma, A7470) was added to 500µl of protein sample diluted to 1µg/µl in IPP buffer (Lysis Buffer 1 but with 5mM EDTA and no Glycerol), and incubated for 4hrs at 4ºC in a small rotator mixer at 4RPM. Beads were spinned for 30sec in a top bench centrifuge, the supernatant removed, and 500µl of IPP buffer added, and rinsed three times. Samples were centrifuged at 12000g for 1min at 4ºC, the supernatant was removed and 40µl of 1.5x Laemmli Buffer was added. Proteins were eluted from the beads by incubating at 95ºC for 5min.

Yeast Transformation: Fresh Y2Gold yeast colony was used to inoculate 3ml of Yeast Peptone Dextrose Adenine (YPDA) liquid media for 8hrs and then 50µl of the culture was used to inoculate 50ml of YPDA and grow over night. The culture was grown until OD^{600} was 0.16 and then centrifuged at 700g for 5min at room temperature. The supernatant was discarded and the yeast resuspended in 100ml of fresh YPDA liquid media. The culture was grown for 3hrs or until OD^{600} reached 0.4-0.5, and centrifuged at 700g for 5min at room temperature, supernatant was discarded and the yeast pellet was resuspended in 60ml of water. Yeast were then centrifuged at 700g for 5min at room temperature, supernatant was discarded and yeast were resuspended in 3ml of 1.1X TE/LiAc (Tris-HCl 1mM, EDTA 1.1mM, Li Acetate 110mM, pH 7.5), centrifuged at 16000g for 15 sec, supernatant was discarded and yeast were resuspended in 1.2ml of 1.1 TE/LiAc. Competent yeast were kept at room temperature and used within less than an hour.

For yeast transformation, herring testis DNA (10µg/µl, Sigma, D-6898) was denatured at 100ºC for 5min and then chilled on ice. Cells were transformed by mixing 50µg of herring testis DNA, 400ng of bait and prey DNA (80ng/µl), 50µl of competent yeast, 500µl of PEG/LiAc (40% Polyethilene glycol (Sigma, P-3640), Lithium Acetate 100mM), vortexing and incubating at 30ºC for 30 min mixing every 10min. After this 20µl of DMSO were added, cells were mixed by inversion, and heat shocked at 42ºC for 15min, mixing every 5min. Cells were then chilled on ice for 2min, centrifuged at 16000g for 10 sec, supernatant was discarded and yeast were resuspended in 200µl of sterile TE 1X. All the yeast were plated on specific dropout selective agar plates (Materials and Methods).

Dong PD, Munson CA, Norton W, Crosnier C, Pan X, Gong Z, Neumann CJ, Stainier DY (2007) Fgf10 regulates hepatopancreatic ductal system patterning and differentiation. Nat Genet 39: 397-402

Field HA, Ober EA, Roeser T, Stainier DY (2003) Formation of the digestive system in zebrafish. I. Liver morphogenesis. Dev Biol 253: 279-90